Available online at www.sciencedirect.com

ScienceDirect

Proceedings of the Combustion Institute xxx (2014) xxx–xxx

Proceedings of the Combustion Institute

www.elsevier.com/locate/proci

Kinetics of the high-temperature combustion reactions of dibutylether using composite computational methods

Mariam J. Al Rashidi [a,*], Alexander C. Davis [b], S. Mani Sarathy [a]

[a] Clean Combustion Research Center, King Abdullah University of Science and Technology, Thuwal, Saudi Arabia
[b] National Institute of Standards and Technology, Gaithersburg, MD, USA

Abstract

This paper investigates the high-temperature combustion kinetics of *n*-dibutyl ether (*n*-DBE), including unimolecular decomposition, H-abstraction by H, H-migration, and C—C/C—O β-scission reactions of the DBE radicals. The energetics of H-abstraction by OH radicals is also studied. All rates are determined computationally using the CBS-QB3 and G4 composite methods in conjunction with conventional transition state theory. The B3LYP/6-311++G(2df,2pd) method is used to optimize the geometries and calculate the frequencies of all reactive species and transition states for use in ChemRate. Some of the rates calculated in this study vary markedly from those obtained for similar reactions of alcohols or alkanes, particularly those pertaining to unimolecular decomposition and β-scission at the α-β C—C bond. These variations show that analogies to alkanes and alcohols are, in some cases, inappropriate means of estimating the reaction rates of ethers. This emphasizes the need to establish valid rates through computation or experimentation. Such studies are especially important given that ethers exhibit promising biofuel and fuel additive characteristics.

Keywords: Dibutyl ether; Combustion; Computational kinetics; Transition state theory

1. Introduction

Over the past few decades, ethers have been the focus of numerous studies due to the wide range of applications associated with these compounds. In addition to being used as industrial solvents, ethers exhibit the potential to enhance combustion and reduce knock in gasoline engines, as well as to reduce the toxicity levels of gasoline exhausts [1] . Moreover, ethers have been identified as promising alternative compression ignition biofuels because of their high cetane number and their oxygen content [2,3].

The oxidation mechanism and kinetics of dimethyl (DME) and diethyl (DEE) ethers are well studied under atmospheric and combustion

* Corresponding author. Address: Clean Combustion Research Center, King Abdullah University of Science and Technology, Al Kindi bldg. level 4, room 4326-WS11, Thuwal, 23955-6900 Jeddah, Saudi Arabia.
E-mail address: mariam.elrachidi@kaust.edu.sa (M.J. Al Rashidi).

http://dx.doi.org/10.1016/j.proci.2014.05.109
1540-7489/

conditions [4–8]. However, few studies exist regarding the oxidation of larger ethers. These include the investigation of the kinetic rates of isomerization of the alkoxyalkylperoxy radicals generated via H-abstraction from C_2 to C_5 ethers by H and OH radicals followed by O_2 addition [9]. Zhou et al. [10] determined the rates of H-abstraction by OH radicals of dimethyl (DME), ethylmethyl (EME) and iso-propylmethyl (IPME) ethers using *ab initio* CCSD(T) calculations coupled to variational transition state and Rice-Ramsperger-Kassel-Marcus (RRKM) theories. Marrouni et al. [11] used the B3LYP/6-311G(d,p) level of theory to investigate the kinetics of H-abstraction from a series of linear symmetrical monoethers by molecular oxygen. Mellouki et al. [12] report the rate constants of the OH-oxidation of dimethyl, diethyl, dipropyl and dibutyl ethers, measured using pulsed laser photolysis-laser induced fluorescence technique in the temperature range 230–372 K. The paucity of reliable kinetic data for ethers has resulted in the lack of a well-defined oxidation mechanism for these compounds. Although the combustion mechanism of DME has been fairly well developed by Curran et al. [5,7,13] and further improved upon by Andersen et al. [14,15], mechanisms of larger ethers continue to be limited. These include a detailed mechanism of the combustion of ethyl methyl, methyl *tert*-butyl and ethyl *tert*-butyl ethers proposed by Yasunaga et al. [16]. Cai et al. [17] recently developed a chemical kinetic model for *n*-dibutyl ether (*n*-DBE) and validated it against first stage ignition delay in a flow reactor and premixed laminar flame speed. In these mechanisms, the rate parameters of elementary reactions pertaining to ethers are taken from the literature, when applicable; otherwise, these parameters are estimated by analogy to similar alkanes or alcohols.

Although analogies are usually effective in providing adequate rate parameter values, estimations can, in some cases, be misleading. This emphasizes the need for well-developed combustion mechanisms of ethers larger than DME, incorporating accurate experimentally or computationally determined rate parameters. With a cetane number of 100 [18], *n*-DBE produced from lignocellulosic biomass is a potentially suitable biofuel or fuel additive for compression ignition engines [19]. A study of the first stage ignition of *n*-DBE in a laminar flow reactor at atmospheric pressure, 10% nitrogen dilution and an equivalence ratio of 0.8 shows that the ignition delay time (IDT) varies between 1.44 and 0.21 s within a temperature range of 470–550 K [20]. Cai et al. [17] show that IDTs of *n*-DBE are approximately 2–4 times less than those of *n*-octane at 20 bar and an equivalence ratio of 1, in the temperature range of 700–1000 K. Moreover, this compound has been shown to produce low levels of soot when it is used as a fuel in diesel engines [18]. The advantages of *n*-DBE as an ignition enhancing and soot reducing blending component have also been demonstrated by Heuser et al. [21] for 2-methyltetrahydrofuran. Considering the established importance of *n*-DBE as a potential biofuel and fuel additive, reliable kinetic data for the elementary combustion reactions of this compound is needed for valid modeling.

In this study, we investigate the rates of unimolecular decomposition and H-abstraction by H and OH from *n*-DBE using computational tools. We also report rates of H-migration and β-scission of the resulting radicals. Figure S1 of supplementary material represents the minimum energy conformer of *n*-DBE, and Fig. 1 illustrates the investigated reactions. This work provides the kinetic parameter values of several important high temperature elementary combustion reactions of *n*-DBE using CBS-QB3 and G4 computational methods.

2. Methods [22]

The temperature dependent kinetic rate constants of the investigated reactions were determined using ChemRate [23] and Gaussian 09 suite of programs [24]. A conformational analysis was conducted using the B3LYP/6-31G(d,p) level of theory to discern the minimum energy conformers of chemical species and transition states. The rotational increments for each dihedral were chosen in such a way that the geometries and energies of all local minima (i.e., gauche and anti-configurations for tetrahedral geometries) were determined. Geometry optimizations and frequency calculations of the resulting minimum energy conformers were performed using B3LYP/6-311++G(2df,2pd). Each transition state was confirmed by the presence of a single imaginary frequency that corresponds to the targeted reaction. Finally, the composite methods CBS-QB3 and G4 were used to calculate the energies of all the optimized species and transition states, excepting those related to H-abstraction by OH

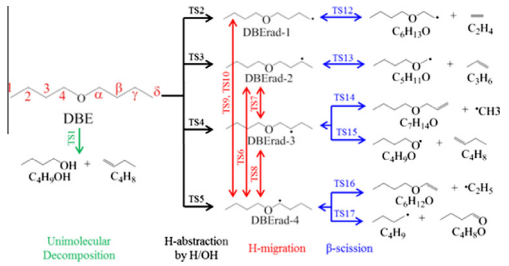

Fig. 1. Investigated high temperature combustion reactions of *n*-DBE.

Please cite this article in press as: M.J. Al Rashidi et al., *Proc. Combust. Inst.* (2014), http://dx.doi.org/10.1016/j.proci.2014.05.109

reactions, which were determined using G3. Isogyric reactions were used in order to enhance the accuracy of the formation enthalpy values used by ChemRate to determine the activation energy of an investigated reaction. The enthalpy of formation of each chemical species and transition state is expressed as the mean of the values determined using a set of three isogyric reactions for both CBS-QB3 and G4. The isogyric reactions are listed in Table S1 of the supporting information.

Rotational barriers were calculated via 10° increment relaxed scans of all rotors at the B3LYP/6-31 + G(d,p) level of theory. Based on the recommendations of Andersson and Uvdal [25], the calculated frequencies were scaled by a factor of 0.9679.

To account for tunneling, the asymmetric Eckart tunneling correction was activated in ChemRate. The use of this feature requires numerical input pertaining to the barrier width of each reaction. This input was supplied through intrinsic reaction coordinate (IRC) calculations at the B3LYP/6-31 + G(d,p) level of theory. In addition to providing barrier width values, IRC computations were used to further confirm the validity of the transition states.

The high pressure limit temperature-dependent rates of the investigated reactions were fit to the three-parameter modified Arrhenius expression $k(T) = AT^n \exp(-E_a/RT)$, in the temperature range 300–2500 K. Thermodynamic properties of all chemical species were also determined and are reported in Table S2 of the supplementary information.

3. Results and discussion

The high temperature reaction classes of *n*-DBE investigated in this work are depicted in Fig. 1. These reactions are comprised of unimolecular decomposition, H-abstraction by H and OH, H-migration, and C—C/C—O bond scission. The potential energy diagrams (PEDs) of the investigated reactions are illustrated in Figs. 2, 4, 6 and 7. The G3 bond dissociation energies (ΔH_R and $\Delta H^{\ddagger}$) of the barrierless *n*-DBE + OH reactions at 298 K are listed in Table 1. The high pressure limit Arrhenius rate parameters, A, n and E_a, are reported in Table 2.

3.1. Unimolecular decomposition

The PED of the unimolecular decomposition reaction of *n*-DBE to give butanol and butene is depicted in Fig. 2. Two possible orientations of the transition state were taken into consideration: (i) TS1-a, where the alkyl groups are on the same side of the planar 4-membered ring transition state conformation, and (ii) TS1-b, which has the alkyl groups on opposite sides of the plane. The total decomposition rate is equivalent to the sum of TS1-a and TS1-b rates. As shown in Fig. 2, the energy difference between the two conformers of TS1 is 0.8 kJ mol^{-1} at 298 K, which is within the uncertainty limit of the CBS-QB3 and G4 computational methods used in this study [26,27]. The fitted value of the activation barrier of unimolecular decomposition of DBE is 276 kJ mol^{-1}, similar to that of the analogous butanol dehydration reaction (273 kJ mol^{-1}) [17]. It is 14 kJ mol^{-1} larger than the MP4/cc-pVTZ//MP2/cc-pVTZ value adopted by Yasunaga et al. [28] for DEE. Considering the differences in the computational methods used to determine the decomposition energies of the two compounds, it is difficult to further discuss the small difference in E_a values. In the DBE combustion mechanism recently developed by Cai et al. [17], the rate of unimolecular decomposition of the fuel was estimated by analogy with the dehydration reaction of butanol to be $k = 10^{14}$-

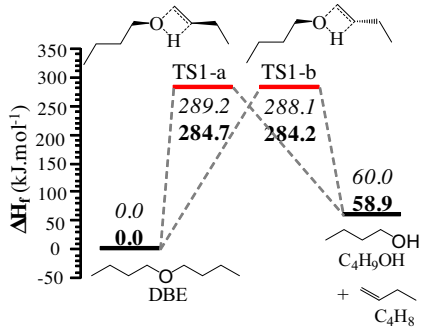

Fig. 2. Potential energy diagram of the unimolecular decomposition reaction of *n*-DBE at 298 K (CBSQB3 values in italics and G4 values in bold).

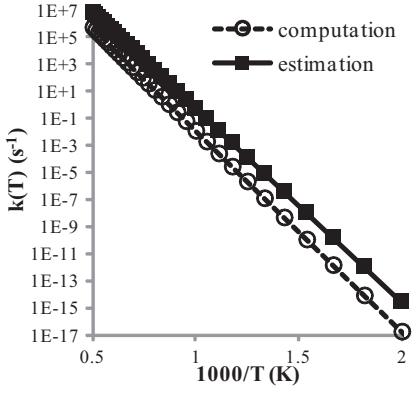

Fig. 3. Comparison of the computational rate of unimolecular decomposition of *n*-DBE (this study) to that estimated by analogy to the dehydration of butanol [17].

Table 1
Bond dissociation energy parameters of H-abstraction by OH of DBE calculated using G3 at 298 K, in units of kJ mol^{-1}.

	Reaction site	ΔH_R G3	$\Delta H^{\ddagger}$ G3
TS18	C1,C9	−79.9	−7.9
TS19	C2,C8	−90.4	−20.5
TS20	C3,C7	−84.5	−15.1
TS21	C4,C6	−105.4	−17.2

exp(−273 kJ mol^{-1}/RT). This analogy overestimates the contribution of the unimolecular decomposition reaction to the degradation of *n*-DBE since it yields rate constants that are 10–100 times greater than those determined computationally in the temperature range 500–2000 K (Fig. 3). In their investigation of *n*-DBE pyrolysis, Enguehard et al. [29] show that butane, butyraldehyde and CO are the main degradation products. Butanol and butene are also detected in the product condensate at concentrations that are 4–20 times less than those of the major products. These results show that *n*-DBE pyrolysis proceeds mainly via homolytic C—O bond cleavage, a reaction that has not been investigated in this study due to the fact that the bond dissociation energy of C—O (321 kJ mol^{-1} [30]) is higher than the activation energy barrier required for the formation of butanol and butene (276 kJ mol^{-1}). Enguehard et al.'s [29] pyrolysis experiments were conducted at low temperatures (250–300 °C) and supercritical pressures (200–2000 bar), conditions that are not directly relevant to combustion. As argued by Enguehard et al. themselves, increasing the pressure promotes addition reactions, thus reducing olefin concentrations. Similarly, butanol decomposition is expected to be faster at higher pressures. Therefore, this data cannot be used to validate the pyrolysis mechanism of *n*-DBE for combustion. Homolytic cleavage dissociation routes of *n*-DBE are less favorable than the decomposition pathway leading to butanol and butane, and thus, have not been investigated in this study.

3.2. H-abstraction

Figure 4 illustrates the PED of the H-abstraction pathways of *n*-DBE by the H-radical. A comparison of the energy values shows that abstraction from the α site is the most thermodynamically and kinetically favorable pathway, followed by abstraction from the γ, β then δ sites. This trend conforms with that of the C—H bond dissociation energies of *n*-DBE [17], and is similar to that observed for alcohols [31,32]. Being barrierless, H-abstraction by OH is clearly quicker and more favorable than H-abstraction by H. The rate parameters of abstraction by OH are not reported herein as they cannot be determined using conventional transition state theory. The 298 K reaction enthalpies (ΔH_R) and activation energies ($\Delta H^{\ddagger}$) of these reactions are listed in Table 1. Both the CBS-QB3 and G4 methods predict the same energy trends for the H-abstraction by H reaction; however, there exists a difference of approximately

Table 2
Arrhenius rate parameters of the investigated reactions fit over the temperature range of 300–2500 K, in units of cm^3, mol^{-1}, s^{-1} and kJ.

	A	n	E_a		A	n	E_a
Unimolecular decomposition				*H-migration*			
TS1-cis	1.2E + 08	1.5	274.9	TS7-EE	7.6E + 04	1.1	60.7
TS1-trans	1.2E + 08	1.3	276.1	TS8-AA	1.1E + 03	1.8	67.4
H-abstraction by H				TS8-AE	9.7E + 01	2.1	66.9
TS2-a	3.3E + 07	1.9	31.8	TS8-EA	3.7E + 02	2.1	66.9
TS2-b	9.2E + 07	1.8	32.6	TS8-EE	8.6E + 02	1.8	67.4
TS2-c	9.4E + 07	1.9	33.9	TS9-A	2.7E + 03	2.1	68.2
TS3-a	8.3E + 07	1.8	20.9	TS9-E	1.4E + 04	1.9	71.5
TS3-b	7.0E + 07	1.8	21.3	TS10-A	1.3E + 03	1.8	50.2
TS4-a	3.2E + 08	1.6	27.6	TS10-E	4.2E + 04	1.3	46.4
TS4-b	6.1E + 07	1.8	25.5	TS11-AA	1.5E + 03	1.4	60.2
TS5-a	6.0E + 07	1.8	13.0	TS11-AE	4.1E + 03	1.3	58.6
TS5-b	7.8E + 07	1.8	13.4	TS11-EA	1.0E + 04	1.3	59.4
H-migration				TS11-EE	1.7E + 03	1.4	62.3
TS6-AA	2.1E + 05	1.2	57.3	*β-scission*			
TS6-AE	1.4E + 05	1.3	51.5	TS12	7.8E + 09	0.8	121.8
TS6-EA	8.6E + 04	1.4	56.9	TS13	4.5E + 08	0.8	113.8
TS6-EE	1.3E + 05	1.3	52.3	TS14	1.9E + 07	1.5	120.9
TS7-AA	8.3E + 04	1.0	61.1	TS15	4.3E + 08	0.8	93.7
TS7-AE	6.8E + 04	1.1	62.3	TS16	2.6E + 10	0.7	126.4
TS7-EA	5.1E + 04	1.1	59.4	TS17	3.6E + 12	0.2	93.7

Please cite this article in press as: M.J. Al Rashidi et al., *Proc. Combust. Inst.* (2014), http://dx.doi.org/10.1016/j.proci.2014.05.109

8–10 kJ between the two sets of values at 298 K, with the CBS-QB3 consistently yielding larger energy values (Table S5 of supplementary information). The rate parameters of abstraction for each H-atom at a particular carbon site are reported separately in Table 2. Seeing as experimental and computational studies on the kinetics of H-abstraction reactions of ethers by H-radicals are scarce, we could only compare the kinetic parameters of H-abstraction from the α position to those determined experimentally by Takahashi et al. [33] for DME in a shock-tube. Their results show that in the temperature range of 300–1500 K, the rate expression for the DME + H reaction is $k = 11.0T^{4.0}\exp(-7.5\ \text{kJ mol}^{-1}/RT)\ \text{cm}^3\ \text{mol}^{-1}\ \text{s}^{-1}$, whereas the rate expression obtained for the α-abstraction in this study is $k = 1.4 \times 10^8 T^{1.8}\exp(-13\ \text{kJ mol}^{-1}/RT)\ \text{cm}^3\ \text{mol}^{-1}\ \text{s}^{-1}$. These two expressions yield rates that are less than one order of magnitude different at temperatures greater than 550 K, with *n*-DBE exhibiting faster rates (Fig. 5). These results are consistent with those reported by Carstensen and Dean [34], who show that the rate of H-abstraction by H from a secondary CH_2 group at the α site in ethanol is greater than that of a primary CH_3 group at the α site in methanol. As expected, the presence of the oxygen atom in *n*-DBE weakens the C—H bonds, resulting in lower activation barriers for H-abstraction by H compared to alkanes.

3.3. H-migration

In this study, only 5, 6 and 7-membered ring transition state H-migration reactions have been investigated. The strain involved in forming transition states with smaller rings is large, leading to high energy barriers, thus rendering these reactions of negligible importance. Similarly, H-migration reactions comprising ring structures with more than 7 atoms are entropically unfavorable due to the additional rotors needed to form the ring. The PED of the H-migration reactions of *n*-DBE studied in this work is illustrated in Fig. 6. The transition marked in blue signifies

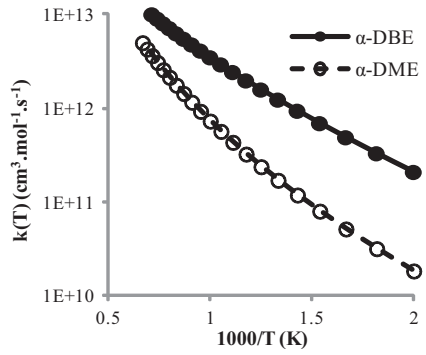

Fig. 5. Comparison of the rates of H-abstraction by H-radical from the α sites of DME [33] and *n*-DBE (rates reported on a per H-atom basis).

the migration between the two β carbon atoms on either side of the oxygen in *n*-DBE. As shown in Fig. 6 and 5-, 6-, and 7-membered ring transition state H-migration reactions have comparable energy barriers varying between 59 and 84 kJ mol^{-1} at 298 K. All possible combinations of axial and equatorial branching of the cyclic transition state structure of each reaction were investigated. Table 2 reports the kinetic rate parameters of the H-migration reactions of *n*-DBE, calculated using different transition state conformations. It is recommended that the rates of different TS conformations be summed up for kinetic modeling purposes.

In order to evaluate the influence of the oxygen atom, the alkyl H-migration rates of *n*-DBE alkyl radicals (DBErads) determined herein are compared to those obtained for the octyl radicals at the CBS-Q and G4 levels of theory [35]. The comparison shows that the difference in energy barriers of migration reactions of DBErads and the octyl radicals is less than 20% for 5-, 6- and 7-membered ring transition state reactions [35]. Both oxygenated and non-oxygenated radicals exhibit higher energy barriers for reactions involving 5-membered ring transition states. Tsang et al.

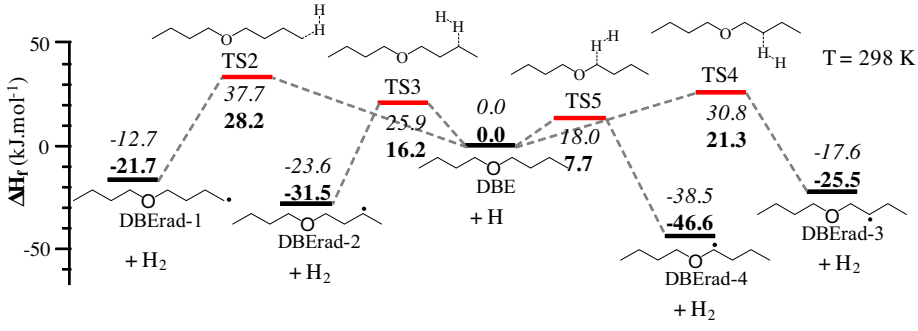

Fig. 4. Potential energy diagram of H-abstraction by H-radical of *n*-DBE at 298 K (CBSQB3 values in italics and G4 values in bold).

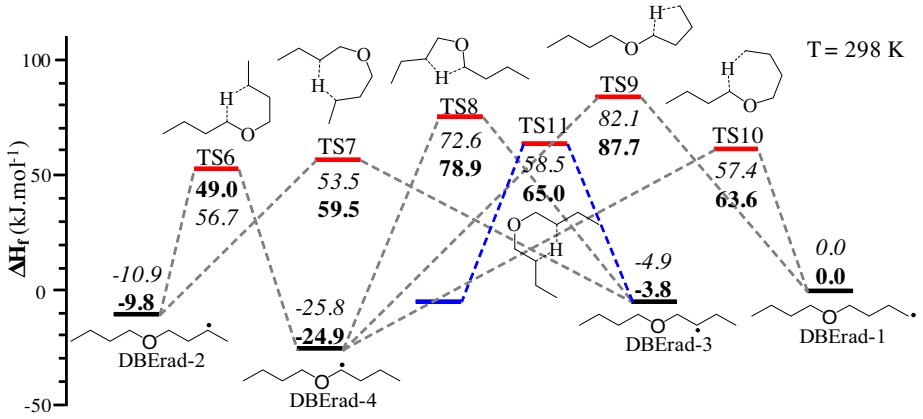

Fig. 6. Potential energy diagram of the 5, 6 and 7-membered ring H-migration reactions of *n*-DBE at 298 K (CBSQB3 values in italics and G4 values in bold).

report experimental rates of octyl radical isomerization reactions [36]. Their activation energies are in good agreement with those determined for *n*-DBE (2–7 kJ difference) except for the α radical (14–22 kJ difference). This is attributed to the stability of the α DBE radical compared to a secondary alkyl radical of octane. Consequently, isomerization rates of α DBErad are 200–4000 times slower than those of the octyl radical.

3.4. β-scission

Another class of high temperature combustion reactions investigated in this study is the β-scission of C—C and C—O bonds in alkyl radicals of *n*-DBE. The PED of these reactions (Fig. 7) shows that the energy barrier of the C—O scission is 97–115 kJ mol^{-1}, whereas that of C—C scission varies between 117 and 129 kJ mol^{-1}. These results are consistent with the bond dissociation energy trend of *n*-DBE reported by Cai et al. [17], and with the energy barriers of C—C and C—O β-scissions of butanol presented by Zhang et al. [32]. At low temperatures (350 K), the C—O scission rates are 3–6 orders of magnitude greater than C—C scission rates, with the route of dissociation of DBErad-4 to give butanal and butyl radical (TS17) being the most kinetically and thermodynamically favorable throughout the investigated temperature range.

The C—C scission reaction rates of DBErads investigated in this study are similar to those reported by Zhang et al. [32] for butanol, with a difference of 1–2, 2–13, and 6–100 times for the δ-γ, γ-β and β-α scissions, respectively. As shown in Fig. 8, the difference in the β-α C—C scission rates of butanol and *n*-DBE is notably high, even at elevated temperatures (up to 2 orders of magnitude). Moreover, the C—O scission rate leading to the formation of the butene from butanol is up to 120 times greater than its analog *n*-DBE scission at high temperatures [32] due to entropic effects. These results indicate that rate estimations of

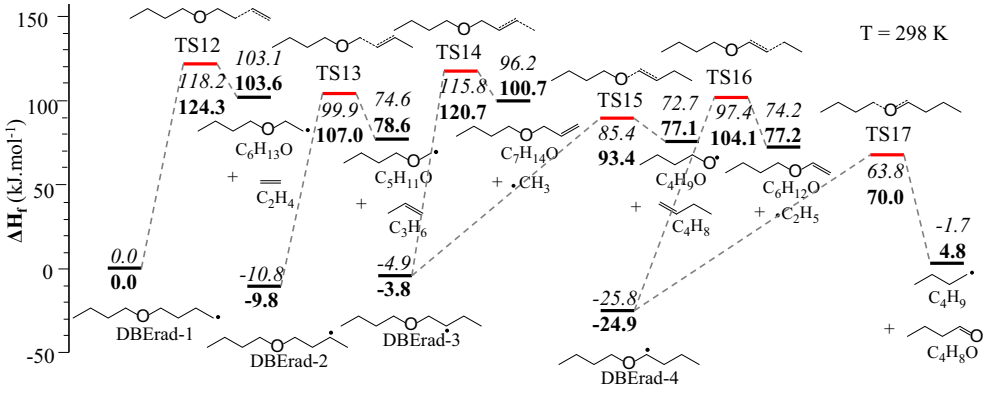

Fig. 7. Potential energy diagram of the C—C and C—O β-scission reactions of the alkyl radicals of *n*-DBE at 298 K (CBSQB3 values in italics and G4 values in bold).

Please cite this article in press as: M.J. Al Rashidi et al., *Proc. Combust. Inst.* (2014), http://dx.doi.org/10.1016/j.proci.2014.05.109

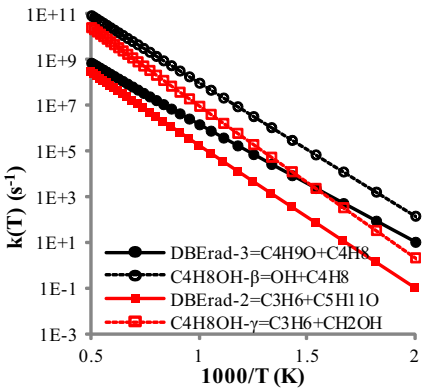

Fig. 8. Comparison of the β-α C—C and C—O bond scission rates of the alkyl radicals of *n*-DBE and butanol [32].

ethers by analogy to alcohols are not always valid, and thus, accurate rate constant measurements for ethers are needed at combustion relevant temperatures.

4. Conclusion

A computational study of the high-temperature combustion reactions of *n*-dibutyl ether was carried out using CBS-QB3 and G4 composite methods for energy computations and B3LYP/6-311++G(2df,2pd) for geometry optimization and frequency calculation. The rate constants of the investigated reactions were determined using conventional transition state theory and corrected for tunneling using the Eckart tunneling correction factor.

The results show that the presence of the oxygen atom in *n*-DBE favors H-abstraction, particularly at the α position. Similar to non-oxygenated alkyl radicals, 5-membered ring H-migration reactions in *n*-DBE are less energetically favorable than those involving 6- and 7-membered ring transition states. Finally, the rates of the C—C and C—O bond scission reactions of the alkyl radicals of *n*-DBE taking place at the α site were determined to be approximately 100 times slower than the butanol counterparts at high temperatures. This indicates that the use of analogy to estimate the rates of combustion reactions of ethers is not always valid. Given the increasing interest in ethers as biofuels and fuel additives, the results obtained in this study emphasize the importance of establishing valid rates of oxidation for these species.

Appendix A. Supplementary data

Supplementary data associated with this article can be found, in the online version, at http://dx.doi.org/10.1016/j.proci.2014.05.109.

References

[1] G.A. Westphal et al., *Toxicology* 268 (3) (2010) 198–203.
[2] Glaude, P.A., et al., *Proceedings of ASME Turbo Expo*, Vancouver, British Columbia, Canada (2011).
[3] K.K. Gupta, A. Rehman, R.M. Sarviya, *Renew. Sust. Energy Rev.* 14 (9) (2010) 2946–2955.
[4] A. Andersen, E.A. Carter, *Mol. Phys.* 106 (2–4) (2008) 367–396.
[5] H.J. Curran, S.L. Fischer, F.L. Dryer, *Int. J. Chem. Kin.* 32 (12) (2000) 741–759.
[6] P. Dagaut, J.-C. Boettner, M. Cathonnet, *Proc. Combust. Inst.* 25 (1) (1996) 627–632.
[7] S.L. Fischer, F.L. Dryer, H.J. Curran, *Int. J. Chem. Kin.* 32 (12) (2000) 713–740.
[8] P.A. Glaude et al., *Combust. Flame* 121 (1–2) (2000) 345–355.
[9] T. Ogura, A. Miyoshi, M. Koshi, *Phys. Chem. Chem. Phys.* 9 (37) (2007) 5133–5142.
[10] C.W. Zhou, J.M. Simmie, H.J. Curran, *Phys. Chem. Chem. Phys.* 12 (26) (2010) 7221–7233.
[11] K. El Marrouni, H. Abou-Rachid, S. Kaliaguine, *Int. J. Quantum Chem.* 108 (1) (2008) 40–50.
[12] A. Mellouki, S. Teton, G. Le Bras, *Int. J. Chem. Kin.* 27 (8) (1995) 791–805.
[13] H.J. Curran et al., *Int. J. Chem. Kin.* 30 (3) (1998) 229–241.
[14] A. Andersen, E.A. Carter, *Isr. J. Chem.* 42 (2–3) (2002) 245–260.
[15] A. Andersen, E.A. Carter, *J. Phys. Chem. A* 107 (44) (2003) 9463–9478.
[16] K. Yasunaga et al., *Combust. Flame* 158 (6) (2011) 1032–1036.
[17] L. Cai et al., *Combust. Flame* 161 (3) (2014) 798–809.
[18] C. Beatrice et al., *Combust. Sci. Technol.* 120 (1–6) (1996) 335–355.
[19] K. Melin, M. Hurme, *Cell. Chem. Technol.* 44 (4–6) (2010) 117–137.
[20] Sudholt, A., et al., Proceedings of the European Combustion Meeting (2011).
[21] B. Heuser et al., *SAE Int. J. Fuels Lubr.* 6 (3) (2013) 922–934.
[22] Certain commercial equipment, i., or materials are identified in this paper to foster understanding. Such identification does not imply recommendation of endorsement by the National Institute of Standards and Technology, nor does it imply that the materials or equipment identified are necessarily the best available for the purpose.
[23] Mokrushin, V., et al. *Chemrate*, v. 1.5.8; NIST Gaithersburg, MD (2006).
[24] Frisch, M.J., et al. Gaussian 09 Revision D.01 Wallingford, CT, 2009.
[25] M.P. Andersson, P. Uvdal, *J. Phys. Chem. A* 109 (2005) 2937–2941.
[26] L.A. Curtiss, P.C. Redfern, K. Raghavachari, *J. Chem. Phys.* 126 (8) (2007) 084108.
[27] J.A. Montgomery et al., *J. Chem. Phys.* 112 (15) (2000) 6532–6542.
[28] K. Yasunaga et al., *J. Phys. Chem. A* 114 (34) (2010) 9098–9109.
[29] F. Enguehard, S. Kressmann, F. Domine, *Adv. Org. Geochem.* 16 (1–3) (1990) 155–160.
[30] D.L. Allara, R. Shaw, *J. Phys. Chem. Ref. Data* 9 (3) (1980) 523–559.

[31] K.A. Heufer et al., *Energy Fuels* 26 (26) (2012) 6678–6685.
[32] P. Zhang, S.J. Klippenstein, C.K. Law, *J. Phys. Chem. A* 117 (9) (2013) 1890–1906.
[33] K. Takahashi et al., *Int. J. Chem. Kin.* 39 (2) (2007) 97–108.
[34] H.-H. Carstensen, A.M. Dean, *Development of Detailed Kinetic Models for the Thermal Conversion of Biomass via First Principle Methods and Rate Estimation Rules*, American Chemical Society, Mines, Golden, Colorado, USA, 2010, pp. 201–243.
[35] A.C. Davis, J.S. Francisco, *Phys. Chem. Chem. Phys.* 14 (4) (2012) 1343–1351.
[36] W. Tsang, W.S. McGivern, J.A. Manion, *Proc. Combust. Inst.* 32 (1) (2009) 131–138.

Please cite this article in press as: M.J. Al Rashidi et al., *Proc. Combust. Inst.* (2014), http://dx.doi.org/10.1016/j.proci.2014.05.109